



Quantifying the Dynamics of Prion Infection: a Bifurcation Analysis of Laurent's Model

EMMANUELLE PORCHER* AND MARINO GATTO†‡

* *Laboratoire Ecologie, Systématique et Evolution, Université Paris-Sud, Bâtiment 362
91405 Orsay Cedex, France* and † *Dipartimento di Elettronica e Informazione and Centro di Studio di
Ingegneria Biomedica-CNR, Politecnico di Milano, Piazza Leonardo da Vinci 32, 20133 Milano, Italy*

(Received on 20 April 1998, Accepted in revised form on 3 April 2000)

Laurent (1996a, *Médecine/sciences* **12**, 774–785; 1996b, *Biochem. J.* **318**, 35–39; 1998, *Bio-phys. Chem.* **72**, 211–222) proposed a model for the dynamics of diseases of the central nervous system caused by prions. It is based on the protein-only hypothesis (Prusiner *et al.*, 1981, *Proc. Natl. Acad. Sci. U.S.A.* **78**, 6675–6679), which assumes that infection can be spread by particular proteins (prions) that can exist in two forms that share the same sequence, but have a different structure. The normal form is harmless, while the infectious isoform of the prion protein catalyses a transconformation from the native isoform to itself within a specialized compartment of the brain cells. This paper systematically explores the model behavior with the aim of quantifying the fundamental parameters characterizing the dynamics of prion infection. To this end we use data from the literature to fix orders of magnitude for the rates of synthesis and degradation of the native form of prion protein and for the shape of the autocatalytic function. The dynamical behavior is classified with respect to two unknown parameters (bifurcation analysis): the rate of spontaneous transconformation and the rate of output of the infectious isoform from the specialized compartment. We thus find that the bistability properties evidenced by Laurent are confined to a certain range of parameters and that permanent oscillations of the two isoforms concentrations are possible. The bifurcation analysis allows us to estimate approximate ranges for the values of the two unknown parameters and consequently to derive incubation times and compare them with actual data for hamster. Also, our study predicts that the output rate of the infectious isoform is relatively insensitive to variations of model parameters.

© 2000 Academic Press

1. Introduction

Prion diseases (Weissmann, 1994) were first diagnosed in the middle of the 18th century, with the discovery of a new kind of disease in sheep: infected animals presented excitability, itching and ataxia due to a degeneracy of the central nervous system which, in the long run, led to paralysis and death. The disease was named scrapie from the

behavior of animals, scraping themselves to relieve itching.

Several diseases, which are all supposed to share a mechanism involving prions, are recognized today. They affect humans, sheep, cows (bovine spongiform encephalopathy better known as BSE), mice and many other species and can be sporadic, genetic or infectious. Human prion diseases include Creutzfeldt–Jacob disease (CJD), Kuru (Gajdusek, 1977), Gerstmann–Sträussler–Scheinker syndrome (GSS) and fatal familial insomnia (FFI). The main characteristics

‡ Author to whom correspondence should be addressed.
E-mail: Gatto@Elet.Polimi.It

of prion diseases are (Caughey & Chesebro, 1997):

- a long incubation period (up to 35 years for humans);
- a degeneracy of central nervous system leading to death;
- neuropathological changes such as neurons death and spongiosis of brain (the prion diseases are also known as transmissible spongiform encephalopathies);
- the absence of immunological response; and
- intra- and inter-specific transmissibility (Aguzzi, 1996; Bruce *et al.*, 1997; Hill *et al.*, 1997).

In 1981 Stanley Prusiner showed that the scrapie agent contained a protein (Prusiner *et al.*, 1981; Prusiner, 1982). This “proteinaceous infectious particle” was named “prion” to distinguish it from conventional transmissible agents such as viruses or bacteria. Prusiner strongly argued that the nature of this agent was one of unexpected properties: it may consist of protein only because no nucleic acid related to the disease has been found up to now (Prusiner, 1991). The component of the prion appears to be an isomeric form of a cellular protein called PrP (prion protein, Dolton *et al.*, 1982; Büeler *et al.*, 1993). The normal form of the protein, PrP^c (cellular) can be found mainly in neuronal cells of either normal or infected individuals, whereas the pathogenic form PrP^{Sc} (scrapie) is only found in the central and/or peripheral nervous systems of infected animals, and is a protease-resistant form of the PrP^c (Kocisko *et al.*, 1994) (the sequences of the two proteins are the same, but the species differ in their secondary structure). The abnormal form PrP^{Sc} associated to BSE and related CJD is not easily degradable (the degradation time constant is not known, but is $\gg 24$ hr according to Borchelt *et al.*, 1990), is exported to the cell surface and can aggregate outside the cell where it might be responsible for the formation of PrP-amyloid plaques in the brain of infected animals (Dolton *et al.*, 1982; Bendheim *et al.*, 1984).

The unusual properties of prions gave rise to a multitude of hypotheses about their nature and ability to spread within the brain of infected individuals. The most credited are the following

(Weissmann, 1994):

- the virus hypothesis considers that a classical viral nucleic acid does exist but has not been isolated yet;
- in the virino hypothesis, the pathogenic agent consists of a nucleic acid encoding itself (it does not encode any protein), recruiting the host PrP^c and changing it into PrP^{Sc} so as to build a proteinic “coat”. The nucleic acid could not be isolated because of the resistance of this proteinic coat;
- the protein-only hypothesis, pioneered by Griffith (1967) and vigorously supported by the work of Prusiner, is the most commonly accepted and suggests that PrP^{Sc} derives from PrP^c thanks to an autocatalytic process: the infectious form PrP^{Sc} can catalyse a transconformation PrP^c \rightarrow PrP^{Sc}. The mechanism through which this occurs might follow a “refolding model” (Prusiner, 1991; Weissmann, 1995), in which PrP^c changes its conformation in the presence of one PrP^{Sc} protein acting as a chaperoning protein, or a “nucleation model” (Jarret & Lansbury, 1993; Kocisko *et al.*, 1995; Weissmann, 1995), in which transconformation occurs when PrP^c binds to a nucleus of PrP^{Sc}.

Relevant mathematical models describing the underlying biochemistry of prion diseases and based on the protein-only hypothesis have been proposed by Kacser & Small (1996), Eigen (1996) and Laurent (1996a,b, 1998) and more recently by Payne & Krakauer (1998) and Nowak *et al.* (1998). Kacser and Small and Laurent showed that a model system based on the autocatalytic process of the protein-only hypothesis exhibits properties of bistability and can exist in two alternative stable steady states. One of them, characterized by its low PrP^{Sc} concentration, can be considered as the state of cells in the brain of a non-infected individual. The other one, because of its high PrP^{Sc} concentration, is thought to be a pathogenic steady state. Changes in the kinetic parameters and/or inoculation of a certain amount of PrP^{Sc} can switch the system from the healthy steady state to the pathogenic steady state. This transition is supposed to be irreversible. Therefore, these models might provide

a simple explanation for the occurrence of prion disease in a single organism by describing the dynamics of prion proteins within a cell (or within the brain of an animal, considered as a homogeneous medium). Payne & Krakauer's (1998) model tries to explain long incubation periods of TSE's by assuming the existence of a bottleneck in the natural protein pathways within the cell. It considers intracellular and surface-bound concentrations of both isoforms and is characterized by bistability too. Nowak *et al.* (1998) assume nucleation as the basic mechanism [see Eigen (1996) for a thorough discussion of the different mechanisms underlying the protein-only hypothesis], from which they derive a model for each cell with three state variables: abundance of PrP^c monomers, abundance of PrP^{Sc} aggregates of monomers and total number of monomers bound in PrP^{Sc} aggregates. The model does not have a bistable behavior and is subsequently used as a fundamental unit in simulation model which considers a two-dimensional array of cells. The authors also present a more sophisticated model for a single cell (five state variables) where PrP^{Sc} aggregation requires a nucleation seed of a certain minimum size. This model instead has bistability properties. In fact, it assumes that all aggregates of monomers below a critical size are unstable and rapidly fall into pieces which convert back to PrP^c. In mathematical terms, there can be three equilibria for the five variables model:

- (1) No monomers or polymers are present.
- (2) Monomers are present, but there are no polymers.
- (3) Both monomers and polymers are present.

Nowak *et al.* (1998) show (by computing basic reproductive ratios) that equilibria (1) and (3) are stable, whereas equilibrium (2) is unstable.

These models correspond to different conceptual mechanisms and their stated goal is to explain prion protein dynamics from a qualitative viewpoint. However, some quantification is required to check whether these models can be accepted as a possible paradigm of reality: some of these mechanisms might not work in reality because they require parameter values that are unrealistic. Unfortunately, very few attempts

have been made to quantify the kinetic parameters of prion infection. The criteria according to which some authors chose numerical values of basic coefficients, such as rates of protein synthesis and degradation, were unclear. As a matter of fact, only the three-dimensional nucleation model by Nowak *et al.* (1998) has been subjected to a quantitative analysis (Masel *et al.*, 1999). In this paper, the authors use experimental data on the initial exponential growth of the disease infectivity to estimate some key parameters of the nucleation model. As their results are quite consistent with published experimental observations, they conclude that nucleation cannot be ruled out on dynamic grounds.

The dynamic behavior of the above models can greatly vary in response to different parameter values. However, this aspect of the problem has not been explored sufficiently (or at all). Indeed, we think that it would be very useful to conduct studies that evidence those parameter values at which the proposed model dynamics undergo qualitative changes. In mathematical terms, these are called bifurcation analyses. Through these analyses the role played by the different parameters in determining, e.g., bistability properties could be clarified.

This paper is a partial response to the needs just outlined. In fact, our goal is to quantify the parameters and explore the dynamic behavior of bistable models of prion infection. As there is no conclusive evidence for the refolding or the nucleation mechanism (Wille *et al.*, 1996), we stick to a simple and rather general model, like the one proposed by Laurent (1996a,b). With reference to this model we have collected the scant available information (data on Syrian Hamsters are used) to fix orders of magnitude for some parameters: the rates of synthesis and degradation of the native form PrP^c and the parameters defining the autocatalytic function. Then we proceed to a complete bifurcation analysis with respect to those parameters that are most uncertain, namely the coefficients regulating the spontaneous formation of PrP^{Sc} from PrP^c in endosomes and the PrP^{Sc} output from endosomes. The analysis reveals that the bistability properties of the system are confined to a possibly narrow range of values for the uncertain parameters and that the model can be

characterized by cyclic fluctuations, a feature which was not evidenced by the previous authors. Using the estimated values of the coefficients of the prion dynamic model, we then proceed to an estimation of both incubation time and the amount of PrP^{Sc} that is produced in endocytic compartments and is exported to the cell surface and outside the cell.

2. Review of Laurent's Models of Scrapie-related Biochemistry

Here we review the models developed by Laurent (1998) to describe prion dynamics. The first model he proposed corresponds to the scheme of Fig. 1. Therefore, the dynamics of the concentration of PrP^c and PrP^{Sc} is given by the equations

$$\frac{d[\text{PrP}^c]}{dt} = v_1 - v_2 - v_3,$$

$$\frac{d[\text{PrP}^{\text{Sc}}]}{dt} = v_3 - v_4,$$

where t is the time, $[\text{PrP}^c]$ and $[\text{PrP}^{\text{Sc}}]$ the concentrations of the different species within a specialized cell compartment (most likely, endocytosis vesicles) and v_i the rate of step i . Step 1 (PrP^c synthesis) is considered as a zero-order kinetic ($v_1 = k_1$, positive constant), because of the constant level of the PrP messenger during a Scrapie infection (Borchelt *et al.*, 1990; Oesch *et al.*, 1995), whereas steps 2 (degradation of PrP^c) and 4 (output of PrP^{Sc} from endosomes) are first order kinetics ($v_2 = k_2[\text{PrP}^c]$) and $v_4 = k_4[\text{PrP}^{\text{Sc}}]$, with k_2 and k_4 being positive constants. The autocatalytic step 3 is a nonlinear process and, although the mechanism of autocatalysis is unknown, the rate of formation of PrP^{Sc} can be described by the following phenomenological equation:

$$v_3 = \frac{a[\text{PrP}^c](1 + rc[\text{PrP}^{\text{Sc}}]^n)}{1 + c[\text{PrP}^{\text{Sc}}]^n},$$

where a, r, n and c are positive constants and $r, n > 1$. The rationale behind this equation is that there is a rate $a[\text{PrP}^c]$ of spontaneous formation of PrP^{Sc} from PrP^c which can be greatly accelerated (up to a factor r) by the presence of PrP^{Sc} . The parameters c and n define the threshold concentration beyond which autocatalysis

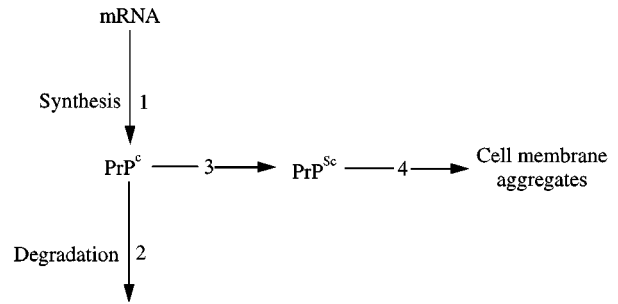


FIG. 1. Metabolism of prion proteins according to the scheme of Laurent's model. The messenger PrP is directly transcribed into the normal isoform PrP^c (step 1) while the pathogenic form PrP^{Sc} originates from the PrP^c , thanks to an autocatalytic mechanism (step 3). PrP^c is also subject to degradation (step 2). PrP^{Sc} is exported to the cell surface and can aggregate outside the cell where it might be responsible for the formation of PrP-amyloid plaques (step 4).

is effective and the steepness of the transition across the threshold. Though the parameters of this equation are purely phenomenological, there are some constraints on their numerical values: a , the coefficient of spontaneous formation of PrP^{Sc} from PrP^c is much smaller (Laurent, 1996b) than the degradation coefficient k_2 , while the acceleration factor r has to be much bigger than unity for autocatalysis to be meaningful. In the case of certain mutations of the PrP gene, a can be increased by orders of magnitude (Laurent & Johannin, 1997).

Given all these kinetics, we can write the differential equations describing the evolution of the concentration of PrP^c and PrP^{Sc} over time:

$$\frac{d[\text{PrP}^c]}{dt} = k_1 - k_2[\text{PrP}^c] - a[\text{PrP}^c] \frac{1 + rc[\text{PrP}^{\text{Sc}}]^n}{1 + c[\text{PrP}^{\text{Sc}}]^n}, \quad (1)$$

$$\frac{d[\text{PrP}^{\text{Sc}}]}{dt} = a[\text{PrP}^c] \frac{1 + rc[\text{PrP}^{\text{Sc}}]^n}{1 + c[\text{PrP}^{\text{Sc}}]^n} - k_4[\text{PrP}^{\text{Sc}}]. \quad (2)$$

Laurent studied the steady states of the system, characterized by constant values of PrP^c and PrP^{Sc} concentrations, and found that, depending on the turnover rate of PrP^c , the system can

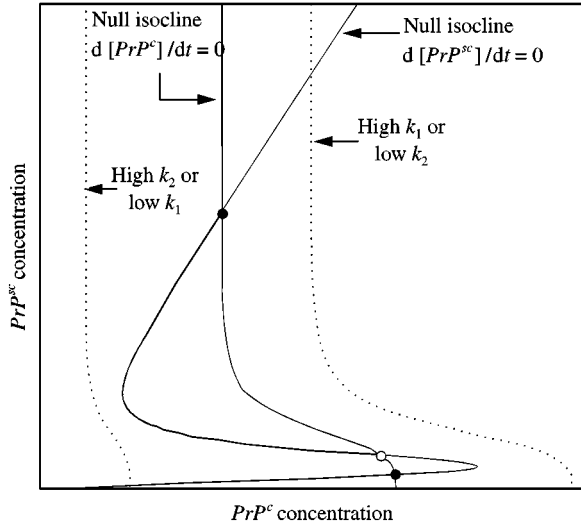


FIG. 2. Null isoclines of the differential system (1), (2) for different values of k_1 and k_2 . The intersection points correspond to the steady states of the system: ● stable, ○ unstable. With intermediate values k_1 and k_2 (corresponding isoclines are displayed as —) two stable equilibria are co-occurring: one is a pathogenic state characterized by a high PrP^{Sc} concentration, while the steady state with the lower PrP^{Sc} concentration is considered a normal equilibrium. (----) indicate how the isocline $d[\text{PrP}^{\text{C}}]/dt = 0$ shifts with increasing or decreasing turnover of PrP^{C} . As a result, one has normal or pathogenic monostability.

possess one or two stable equilibria: a normal one with low PrP^{Sc} concentration and a pathogenic one with high PrP^{Sc} concentration. In fact, the null isoclines $d[\text{PrP}^{\text{C}}]/dt = 0$ and $d[\text{PrP}^{\text{Sc}}]/dt = 0$ are two curves, respectively, given by the equations

$$[\text{PrP}^{\text{C}}] = \frac{k_1(1 + c[\text{PrP}^{\text{Sc}}]^n)}{k_2 + a + c[\text{PrP}^{\text{Sc}}]^n(k_2 + ar)}, \quad (3)$$

$$[\text{PrP}^{\text{C}}] = \frac{k_4[\text{PrP}^{\text{Sc}}](1 + c[\text{PrP}^{\text{Sc}}]^n)}{a(1 + rc[\text{PrP}^{\text{Sc}}]^n)}. \quad (4)$$

The shape of the isoclines in the positive quadrant is portrayed in Fig. 2. There is generically an odd number of intersections (steady states) between the two curves, although, with the range of parameters used by Laurent, there are no more than three. When this is the case (isoclines represented by solid lines in Fig. 2) the intermediate equilibrium is a saddle, namely a steady state attracting along a certain direction and repelling

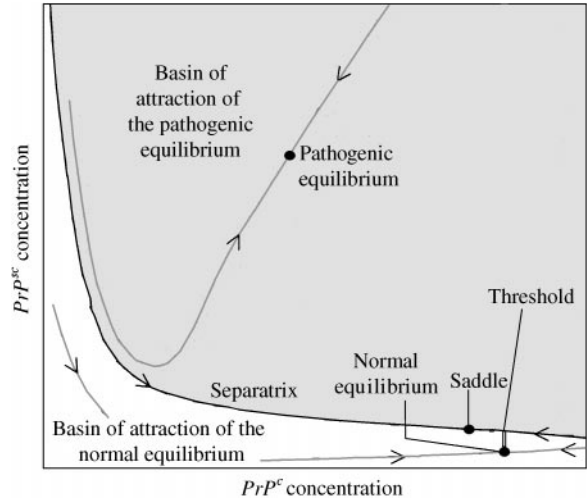


FIG. 3. Basins of attraction of the two stable equilibria of Laurent's model when the system exhibits properties of bistability. The state of the system can be in either a normal equilibrium (characterized by a low PrP^{Sc} concentration) or a pathogenic equilibrium (characterized by a high PrP^{Sc} concentration). The basins are separated by the stable manifold of the saddle (*separatrix*). During an infection, the separatrix acts as a threshold: the disease cannot develop unless the increase of PrP^{Sc} concentration drives the system from the normal equilibrium beyond this threshold and into the basin of attraction of the pathogenic equilibrium.

along another direction, while the other intersections define the normal and the pathogenic equilibria. From these results, Laurent proposed two different explanations for the occurrence of infectious or sporadic prion diseases:

1. The development of the disease after a contamination by PrP^{Sc} depends on the added quantities of PrP^{Sc} in the cell (or in the brain). In fact, as shown in Fig. 3, the phase plane ($[\text{PrP}^{\text{C}}]$, $[\text{PrP}^{\text{Sc}}]$) is partitioned by the separatrix associated with the saddle equilibrium into two regions, which correspond to the basins of attraction of two stable equilibria. The contamination of a cell in a normal state will not induce the disease as long as the state of the system is not kicked into the basin of attraction of the abnormal equilibrium. But if an inoculum of PrP^{Sc} brings the state of the system beyond a threshold, which is represented by the separatrix, the disease will develop.

2. As the bistability properties depend on the turnover rate of PrP^{C} (as shown in Fig. 2 where

dashed lines correspond to the isocline $d[PrP^c]/dt = 0$ for high and low turnover), the occurrence of sporadic diseases could be due to a modification of this turnover rate, namely to an increase of k_1 or a decrease of k_2 . This change in PrP^c dynamics would make the system shift from bistability to pathogenic monostability, and “the very slow accumulation of the abnormal form of the protein in the brain could in fact be the consequence and not the cause of the disorders” (Laurent, 1996b).

Considering that the biochemistry of the autocatalytic step is not well known and is described in a phenomenological way, alternative nonlinear autocatalytic equations may be used to model the conversion of PrP^c and PrP^{Sc} . Another model by Laurent (1998) is in fact based on the same scheme as the first one, but differs in the way the rate of formation of PrP^{Sc} from PrP^c is described:

$$v_3 = k_{spont}[PrP^c] + \frac{k_{cal}[PrP^c]}{K_M + [PrP^c]}[PrP^{Sc}]$$

with k_{spont} , k_{cal} and K_M being positive constants. The spontaneous rate of formation of PrP^{Sc} is a first-order kinetic while autocatalysis is now additive and corresponds to the nonlinear term. The rationale behind this latter term is that PrP^c acts as a substrate and the dimeric form of the scrapie isoform acts as a catalyst. Another functional form was used by Kacser & Small (1996), whose model has the further hypothesis that PrP^{Sc} does not originate directly from PrP^c , but from an intermediately species of PrP , which has not been experimentally evidenced yet.

The study of this further model by Laurent (1998) shows that the system exhibits bistability properties that are similar to those already evidenced: the protein concentrations can be in either a normal or a pathogenic equilibrium. In other words, the second model does not possess any new dynamical property. For this reason, since the biochemistry of autocatalysis is not known in such a detail as to make us incline towards a particular equation, we will from now on concentrate our attention on the study of eqns (1) and (2).

3. Bifurcation Analysis

In this section, the dynamical system described by eqns (1) and (2) will be subjected to a bifurcation analysis (Kuznetsov, 1995), namely to a mathematical study that points out for which parameter values the model dynamics undergoes qualitative changes. To simplify notation, we will from now on set $X = [PrP^c]$ and $Y = [PrP^{Sc}]$. The model is therefore described by the equations:

$$\frac{dX}{dt} = k_1 - k_2X - aX \frac{1 + rcY^n}{1 + cY^n}, \quad (5)$$

$$\frac{dY}{dt} = aX - aX \frac{1 + rcY^n}{1 + cY^n} - k_4Y. \quad (6)$$

Model (5), (6) is identified by seven parameters, the actual values of which determine the dynamical behavior of the system. Despite the simplicity of the model a bifurcation analysis with respect to all of them is practically impossible. Therefore, we try to improve on past approaches by exploiting the existing experimental evidence to attribute reasonable values (or ranges of values) to some parameters and thus restrict the bifurcation analysis to a few of them.

Data concerning protein concentration in the brain of healthy or infected hamsters are given by Meyer *et al.* (1986), Prusiner *et al.* (1990) and Prusiner (1991, Table 1). Another information we may use is the estimation of the coefficient of degradation of PrP^c , given by Borchelt *et al.* (1990): $k_2 = 0.13 \text{ hr}^{-1}$. From this value and the concentration of PrP^c in the brain of normal hamsters, we derive an estimation of the rate of synthesis of PrP^c (k_1). In fact, in the brain of a non-infected animal, we may consider that $Y \approx 0$ and the dynamics of prion is simply given by

$$\frac{dX}{dt} = k_1 - k_2X.$$

At equilibrium we thus have $[PrP^c]_{eq} = k_1/k_2$. As $1 \mu\text{g g}^{-1} < [PrP^c]_{eq} < 5 \mu\text{g g}^{-1}$, we obtain a range of values for k_1 : $0.13 \mu\text{g g}^{-1} \text{ hr}^{-1} < k_1 < 0.65 \mu\text{g g}^{-1} \text{ hr}^{-1}$. We choose $k_1 = 0.5 \mu\text{g g}^{-1} \text{ hr}^{-1}$ as a reference value for the bifurcation analysis. It should be remarked that this is not

TABLE 1
Concentrations (μg of PrP protein per grams of brain tissue) of cellular and scrapie PrP isoforms in Syrian hamster brains

	PrP ^c ($\mu\text{g g}^{-1}$)	PrP ^{Sc} ($\mu\text{g g}^{-1}$)
Concentration in normal Syrian hamster brain	$\approx 1-5$	—
Concentration in scrapie-infected Syrian hamster brain	$\approx 1-5$	≈ 5 to 10

a limitation because the system can be rescaled with respect to k_1 by taking X/k_1 and Y/k_1 as new state variables. Therefore, all the bifurcation diagrams we will obtain can be simply referred to other values of k_1 by suitable rescaling.

The use of the available data on the concentration of PrP^{Sc} in infected animals is more critical. In fact, the concentration of the abnormal form of PrP in the brain of an infected hamster ($5 \mu\text{g g}^{-1} < Y < 10 \mu\text{g g}^{-1}$) is the figure found at the onset of the disease, i.e. approximately 70 days after inoculation. At that time the disease has spread to a large part of the brain tissues. We have thus assumed that this figure is an approximate indicator of PrP^{Sc} local concentration at equilibrium. This concentration may underestimate the cellular concentration used in our model, since it has been measured in brain homogenates that include also uninfected parts of the brain. On the other hand, the concentration of PrP^{Sc} in brain homogenates also accounts for extracellular aggregated PrP^{Sc}, which might counterbalance the previous underestimation. We can thus suppose that the value of $5-10 \mu\text{g g}^{-1}$ gives a good order of magnitude for the local cellular concentration of PrP^{Sc}. In this sense, it can be used to determine ranges for parameters c and n , which define the threshold concentration of PrP^{Sc} for autocatalysis to be effective. More precisely, let $f(Y) = (1 + rcY^n)/(1 + cY^n)$ be the factor that multiplies the rate of spontaneous conversion from PrP^c to PrP^{Sc}. This autocatalytic term corresponds to a sigmoid curve, whose inflection point is $Y_i = \sqrt[n]{(n-1)/c(n+1)}$ and which saturates to r for large values of Y . Therefore, $f(\cdot)$ is practic-

ally equal to unity for concentrations much smaller than Y_i , whereas it practically equals r for concentrations much higher than Y_i . The exponent n determines the rapidity of transition from no autocatalysis to full autocatalysis — larger n corresponds to a steeper $f(\cdot)$ at Y_i . It is reasonable to assume that within the range of $[PrP^{Sc}]$ ($5 \mu\text{g g}^{-1} < Y < 10 \mu\text{g g}^{-1}$) the factor $f(\cdot)$ should be large enough for an efficient autocatalysis to take place, but should not be saturated, otherwise the dynamics would become linear and the model would not be effective in describing the disease insurgence. Therefore, we will set a lower ($2 \mu\text{g g}^{-1}$) and an upper bound ($8 \mu\text{g g}^{-1}$) for the value of the inflection point and conduct our analysis in correspondence to these two values. By setting Y_i , we constrain c to depend on n as follows:

$$c = \frac{n-1}{Y_i^n(n+1)}. \tag{7}$$

Up to now, we have eliminated three degrees of freedom and are left with four parameters with respect to which the bifurcation analysis can be performed: the exponent n , the saturation level r , the spontaneous conversion coefficient a and the PrP^{Sc} output coefficient k_4 . We have decided to concentrate our attention on a and k_4 because of their biological importance. Therefore, we have chosen to run a bifurcation analysis in the parameter plane (k_4, a) for a few selected values of n and r . The range of n is assumed to be 2–6 and that for r to be 4–400 [Laurent (1996a) used $n = 4$ and $r = 40$]. The analysis will show that, for any r and n , the bistability properties of the prion system are confined to a range of values of k_4 and a .

The bifurcation curves presented in this section have been computed by means of LOCBIF, a program implementing a powerful continuation technique for bifurcation analysis (Khibnik *et al.*, 1993). Figure 4(a) provides an idea of the kind of bifurcation diagram which characterizes the model. It corresponds to some “typical” values for the parameters: inflection point = $2 \mu\text{g g}^{-1}$, $n = 4$, $r = 40$. We have chosen these values, because in this way we obtain a reference diagram which includes all the possible bifurcations for the model we are considering. We can thus draw comparisons between that diagram

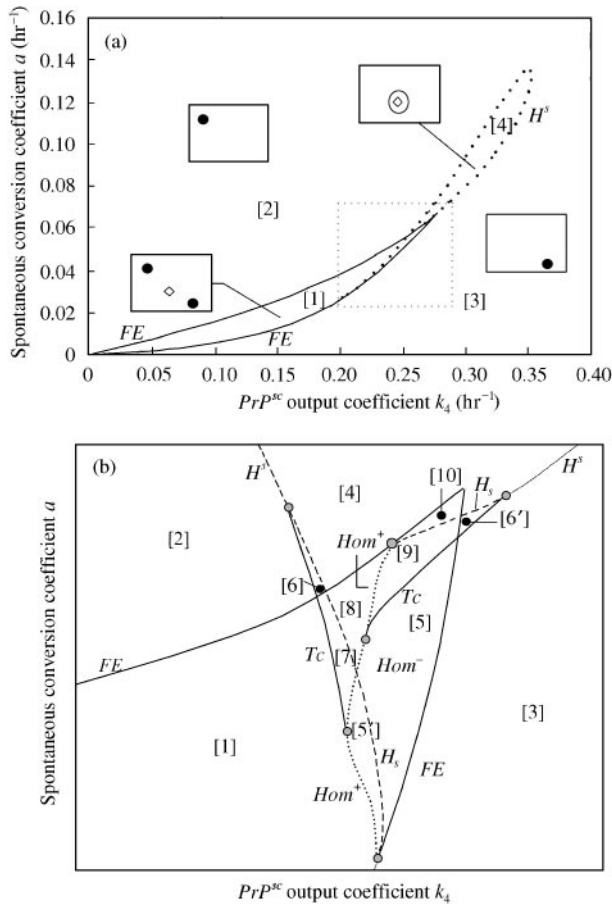


FIG. 4. Bifurcation diagram of Laurent's model with respect to the PrP^{Sc} output coefficient (k_4) and the spontaneous conversion coefficient (a). k_1 and k_2 are set to their reference values and $n = 4$, $c = 0.0375$, $r = 40$. (a) Simplified bifurcation diagram showing only fold bifurcations of equilibria and supercritical Hopf bifurcations. Regions [1]–[4] are characterized by sets of invariants qualitatively described in the corresponding windows (nodes, \bullet , saddles, \diamond ; and \odot , cycles). (b) Magnification of the dotted window in Fig. 4(a), showing the complete bifurcation diagram of the system with respect to a and k_4 . FE , H^s , H_s , Hom , Tc indicate, respectively, fold bifurcation of equilibria, supercritical and subcritical Hopf bifurcations, homoclinic bifurcations of stable and unstable cycles and tangent bifurcations of cycles. For the sake of comprehension, regions [5]–[10] have been made much bigger than they actually are. Regions [1]–[4] are the same as in Fig. 4(a). Region [5] is characterized by a normal stable equilibrium, a pathogenic unstable equilibrium and a saddle, while region [5'] is similar, but the pathogenic equilibrium is stable and surrounded by a small unstable cycle. In regions [6] and [6'], one stable (respectively, pathogenic and normal) equilibrium is surrounded by one unstable and one stable cycle. Regions [7]–[10] are characterized by a stable cycle surrounding two nodes (one stable and one unstable), a saddle, and possibly an unstable cycle.

and the ones plotted with different values of Y_i , n and r . Figure 4(a) is actually a simplified version of the bifurcation diagram, because some bifurca-

tion curves are so close that they have been consolidated. For this reason Fig. 4(b) shows a magnification of the window evidenced in Fig. 4(a) and reports the complete bifurcation diagram. The bifurcation curves are identified by the following symbols:

- FE Fold bifurcation of equilibria: along these curves one stable and one saddle equilibrium collide and vanish.
- H^s Supercritical Hopf bifurcation: along these curves a stable cycle is born from a stable equilibrium.
- H_s Subcritical Hopf bifurcation: along these curves an unstable cycle is born from an unstable equilibrium.
- $Hom-$ Homoclinic bifurcation for stable cycles: along these curves a stable cycle collides with a saddle and vanishes.
- $Hom+$ Homoclinic bifurcation for unstable cycles: along these curves an unstable cycle collides with a saddle and vanishes.
- Tc Tangent bifurcation of cycles: along these curves one stable and one unstable cycle collide and vanish

The bifurcation curves are the boundaries of different regions, indicated by numerals included in square brackets. Regions [5]–[10], eliminated from Fig. 4(a) because they are very small, are shown in the enlargement. Each region corresponds to a particular set of invariants (equilibria and cycles) specified in the caption to Fig. 4. In region [1], characterized by low values of both a and k_4 , the system exhibits properties of bistability, with a normal and a pathogenic equilibrium both being stable. In region [2], characterized by high a and low k_4 the pathogenic equilibrium is the only steady state, because the saddle and the normal equilibrium have vanished via a fold bifurcation. In region [3], characterized by low a and high k_4 , only the normal equilibrium exists, because the saddle and the pathogenic equilibrium have vanished via another fold bifurcation. In region [4], characterized by intermediate values of both the rate of PrP^{Sc} output from endosome and the rate of spontaneous conversion, a kind of dynamics not evidenced by the previous studies appears: there are no stable

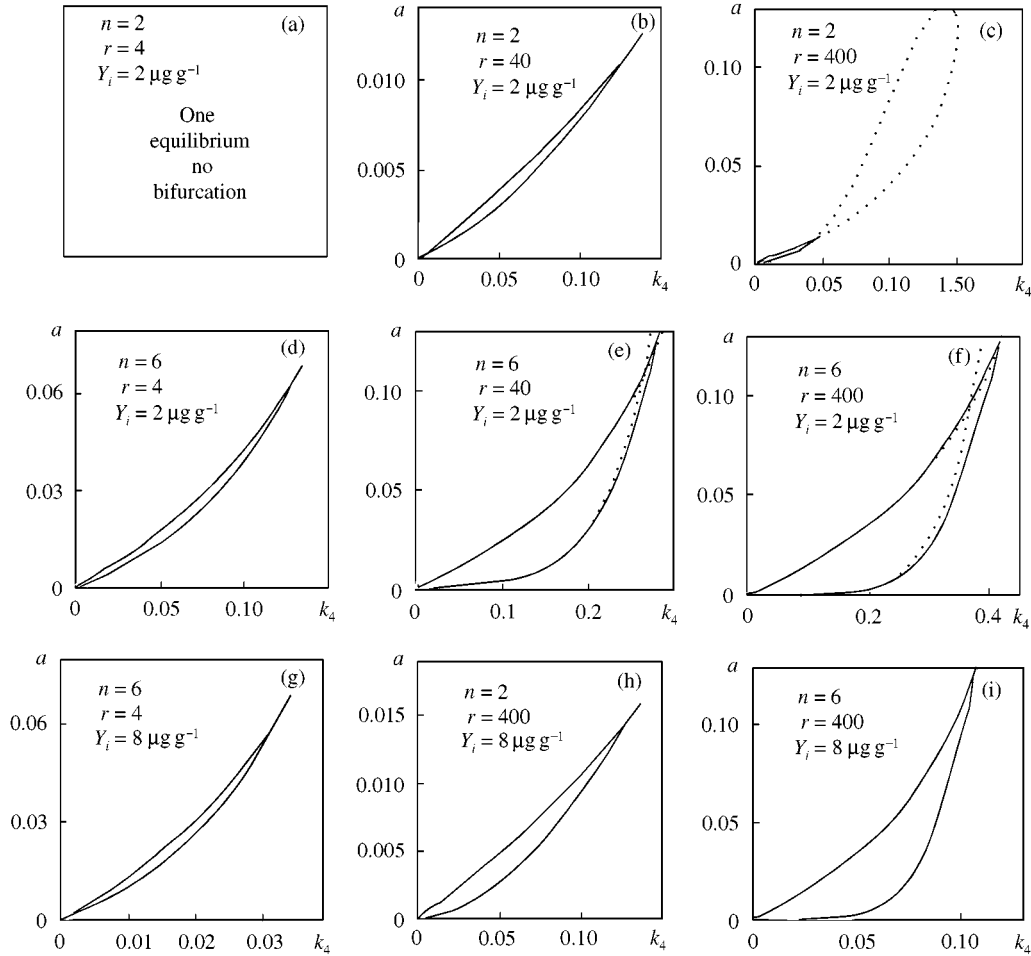


FIG. 5. Simplified bifurcation diagrams with respect to the output coefficient (k_4) and the spontaneous conversion coefficient (a). The figure shows the influence of the inflection point Y_i , the saturation level r and the exponent n on the existence and shape of the bifurcation curves. Dashed curves identify Hopf bifurcations while solid lines correspond to fold bifurcations of equilibria. The rates of synthesis (k_1) and degradation (k_2) of PrP^c are set to their reference values. (a)–(f) correspond to an inflection point of $2 \mu\text{g g}^{-1}$, while for (g)–(i) the inflection point is $8 \mu\text{g g}^{-1}$. The value of c depends on n as shown in eqn (7). When the inflection point is $8 \mu\text{g g}^{-1}$, there is no bifurcation for $n = 2, r = 4$.

equilibria, but there is a limit cycle and therefore the concentration of prion proteins undergoes cyclic fluctuations. The cycle is born via a supercritical Hopf bifurcation from either a normal or a pathogenic equilibrium.

Figure 5 shows the influence of the parameters determining the intensity of autocatalysis (namely the inflection point Y_i , the saturation level r and the exponent n) on the existence and shape of bifurcation curves. Although values of a and k_4 are not known, upper bounds for both parameters have been established. As a is known to be much smaller than $k_2 = 0.13 \text{ hr}^{-1}$, this value has been used as an upper bound. As for k_4 , its upper

bound is suitably adjusted so that all bifurcation curves within the range of a are included. A first remark that emerges from analysing Fig. 5 is that a lower value of the inflection point [Fig. 5(a)–(f)] corresponds to a greater variety of the bifurcation diagrams. In particular, for small values of r and n ($r = 4$ and $n = 2$), there is no bifurcation, because there exists only one equilibrium. This equilibrium may be defined as normal for high values of PrP^{Sc} output rate or small values of the spontaneous rate of PrP^{Sc} formation and pathogenic for low k_4 or high a . On the contrary, for strong ($r = 400$) and highly nonlinear ($n = 6$) autocatalysis, both oscillations and bistability of

equilibria are possible. Increasing r from 4 to 400 brings about oscillations, while increasing n from 2 to 6 has the effect of augmenting the parameter region where bistability occurs. When we assume a higher inflection point [$8 \mu\text{g g}^{-1}$, Fig. 5(g)–(i)], we see that no oscillations are possible. For low values of the strength of autocatalysis ($r = 4$) only high n yields a (small) bistability region. For $r = 400$, bistability is restricted to a small area in the parameter space for low n , yields a (small) bistability region. For $r = 400$, bistability is restricted to a small area in the parameter space for low n , whereas $n = 6$ corresponds to a wider area of bistability.

4. Discussion

In this paper, we have explored and quantified the dynamics of prion proteins within the brain of an individual by means of a mathematical model [eqns (5) and (6)] developed by Laurent. This author let the turnover of PrP^c vary for a given set of the other parameters and investigated the response of the model to this variation. Contrary to what he did, we have estimated k_1 and k_2 from the literature and have instead studied the influence of the parameters defining autocatalysis and exit of the scrapie isoform from a cellular specialized compartment. To this end, we have run a bifurcation analysis of the model with respect to the two biochemical parameters (the spontaneous conversion coefficient and the PrP^{Sc} output coefficient, a and k_4) that seem to be most critical, as there is very little experimental information on their ranges. We have shown that the bistability properties evidenced by Laurent and Kacser and Small are often confined to a rather small range of values for these two parameters. This seems to point out that of the two mechanisms postulated by Laurent for the insurgence of the disease (contamination from PrP^{Sc} in a bistable system or modification of some structural parameters that make the system shift to pathogenic monostability) it is the latter that seems to be most likely for scrapie-infected hamsters. More precisely, a reduction of the PrP^{Sc} output rate or an increase in the rate of spontaneous formation of PrP^{Sc} might bring the system from region [3] (or [1]) to region [2] and, as a result, trigger the development of the disease. While the influence of the

rate of spontaneous formation of PrP^{Sc} was predictable (the more PrP^{Sc} is synthesized, the less probable is the existence of a normal equilibrium), the effect of a small rate of output of the scrapie isoform from a brain cell may appear somehow surprising. The rationale behind this effect is as follows: lower values of k_4 imply a higher concentration of PrP^{Sc} and this, in turn, greatly accelerates autocatalysis, thus creating pathogenic monostability. Our bifurcation diagram has also revealed the existence of cyclic dynamics, which were not evidenced by previous analyses. It remains to be seen whether they can play an important role in practice, because the size of the cycles is rather small (this has been shown by extensive simulation) and oscillations can be found only for particular values of a and k_4 . The experimental confirmation of the existence of oscillations would certainly be hindered by difficulty in collecting the relevant data. Also, it is quite possible that the existence of oscillations depends on the model we have chosen, which is purely phenomenological.

It is worth noticing that from Fig. 5 one can infer that either mechanism of disease insurgence can operate only for values of $k_4 < 0.5 \text{ hr}^{-1}$, because for greater values no catastrophic bifurcation curve is crossed by varying a or k_4 . Actually, we can further restrict the range of values for k_4 because it can be actually shown that the pathogenic equilibrium (high PrP^{Sc} concentration) is really distinct from the normal one (low PrP^{Sc} concentration) in the lower part of the regions of bistability. Thus, we can very roughly set an upper bound of 0.1 hr^{-1} for the rate of PrP^{Sc} output from the specialized compartment. We thus see how the bifurcation analysis provides a way to approximately estimate a basically unknown parameter.

A fundamental problem that can be addressed by using the parameter values so far estimated is that of incubation times, which are known to be quite long (from a few days to many years for human TSEs). Laurent (1996b) found that the shift to the pathogenic equilibrium is a very rapid step (the order of seconds). His result, however, is clearly due to the inappropriate choice of parameter values. We have therefore estimated the time required to go to a pathogenic state with our set of parameters. The infection has been

TABLE 2

Comparison between the time required to reach the model pathogenic state and available data of the incubation period of scrapie in hamsters (Prusiner, 1991; Weissmann, 1994)

Parameters	Initial PrP ^{Sc} concentration (μg g ⁻¹)	Amount of PrP ^{Sc} added in brain (inoculum) (μg g ⁻¹)	Estimated time required to go to pathogenic state (days)
$Y_i = 2, n = 2, r = 400, a = 7 \times 10^{-4}$	0.06	0.5	6 9
$Y_i = 2, n = 4, r = 40, a = 5 \times 10^{-3}$	0.4	0.8	3 5
$Y_i = 2, n = 4, r = 400, a = 10^{-3}$	0.08	1	3 No disease
$Y_i = 2, n = 6, r = 40, a = 10^{-2}$	0.8	0.3	3 3
$Y_i = 2, n = 6, r = 400, a = 5 \times 10^{-3}$	0.4	0.5	3 4
$Y_i = 8, n = 2, r = 400, a = 4 \times 10^{-3}$	0.4	1.22	9 5-6
$Y_i = 8, n = 6, r = 400, a = 10^{-2}$	0.7	3.9	2-3 No disease
Experimental data (hamster)	≪ 1	?	50-100

Note: We simulate an infection either through an inoculum or an increase of the spontaneous conversion rate $a (\times 2)$. Numbers in bold correspond to the latter mechanism. We set $k_4 = 0.05 \text{ hr}^{-1}$, while values for a were chosen so as to obtain bistability. k_1 and k_2 were set to their reference values.

simulated according to the two different insurgence mechanisms as follows: (1) given the concentrations of PrP^c and PrP^{Sc} at the normal equilibrium, we have increased the initial concentration of PrP^{Sc} so as to exceed the threshold (given by the separatrix, shown in Fig. 3) by 10% and then we have calculated the time required for the system to go to the pathogenic equilibrium ($\pm 10\%$); and (2) given the concentrations of PrP^c and PrP^{Sc} at the normal equilibrium for a certain value of a , we have doubled a and then we have calculated the time required for the system to go to the pathogenic equilibrium ($\pm 10\%$) corresponding to the new value of a . The results, provided in Table 2, show that this time, although on a correct scale of days instead of seconds, is much shorter than the measured incubation period of scrapie in hamsters.

However, it should be remarked that reaching the pathogenic equilibrium at the cellular level does not mean that the first disorders associated with prion diseases will appear immediately. In fact, incubation times are measured as the time elapsed between inoculum of infected brain and development of clinical signs of scrapie, but the accumulation of PrP^{Sc} begins much earlier. As

reported by De Armond *et al.* (1992), PrP^{Sc} is first detected in the thalamus of Syrian hamsters about 15 days after inoculation. It then spreads to septum, neocortex and finally caudate nucleus after c. 60 days. At this time the first clinical signs of scrapie begin to appear. We do not know if the neurological dysfunctions are due to the accumulation of PrP^{Sc} in the brain or its aggregation into amyloid fibrils or the lack, in the long run, of functional PrP^c [see the article by Brown *et al.* (1997) on the role of PrP^c in regulating copper in cell membranes]. Although the period between the time when Laurent's model reaches the so-called pathogenic equilibrium and the first observation of actual pathological changes is quite long, the predictions of Table 2 are not so unrealistic, if one considers that the model is intended to describe the cellular level or a brain considered as a homogeneous medium (which is not in reality).

If we formulate the hypothesis that the disease becomes full-fledged because of the effect of neurotoxic aggregates, we can use the model to estimate the amount of PrP^{Sc} that is exported to the cell surface and might, at least in part, aggregate outside the cell. Figure 6 shows how the rate of

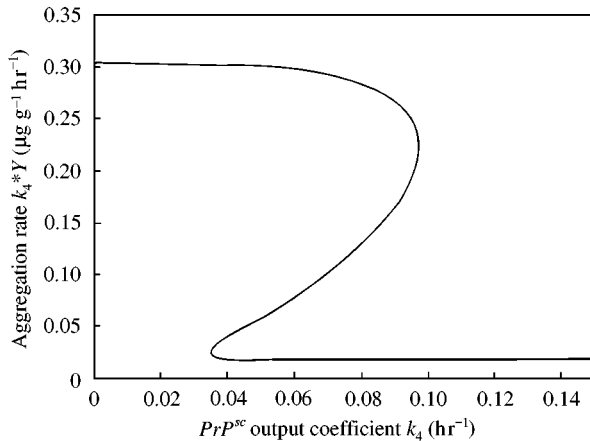


FIG. 6. Output rate of PrP^{Sc} ($k_4 Y$) at equilibrium as a function of the output coefficient k_4 , when $n = 4$, $r = 40$, $Y_i = 2 \mu\text{g g}^{-1}$ and $a = 0.05 \text{ hr}^{-1}$. k_1 and k_2 are set to their reference values.

output of PrP^{Sc} ($k_4[\text{PrP}^{\text{Sc}}]$) at equilibrium varies with k_4 itself. It is interesting to remark that the rate is remarkably constant up to values of k_4 quite close to the fold bifurcation. If we let parameters other than k_4 vary, the rate of aggregation changes accordingly but the range is not very wide: between 0.2 and $0.5 \mu\text{g g}^{-1} \text{ hr}^{-1}$. If there were an experimental way to distinguish between intracellular and extracellular PrP^{Sc} , this prediction might be tested. Unfortunately, we have not been able to find data that could be usefully compared with our guess.

5. Concluding Remarks

The model of prion infection we have analysed is extremely crude, as it neglects a precise description of underlying biochemistry and considers only the cellular level or the brain as a homogeneous medium. There is no doubt that more realistic models could be utilized to explore the dynamics of prion disease in greater detail. In particular, including spatial effect seems of the greatest importance. However, even if we restrict our attention to the central nervous system and neglect the problem of diffusion from peripheral tissues to the brain, this would require an explicit description of both axonal transport and diffusion through the extracellular compartment. Unfortunately, no quantification is possible, as of now, for the transmission rate from cell to cell. Also, it is not clear up to now whether amyloid

aggregates in the extracellular space can be instrumental in spreading infection (Wille *et al.*, 1996). Therefore, building realistic spatial models is quite problematic at the moment. An attempt has been made through the simulation of a cellular array by Nowak *et al.* (1998), but more work is necessary to obtain convincing models. Indeed, it is the very simplicity of Laurent's model that has allowed us to roughly estimate some basic and previously unknown parameters of the infection dynamics. As more and more data on prion disease become available, calibration of more sophisticated models will be possible. In the meanwhile, this is the best we could achieve with the existing experimental evidence. It is interesting to remark how bifurcation analysis, a mathematical tool that is usually considered apt only for qualitative assessments of a model dynamic behavior, could help us derive quantitative results too.

Up to now, epidemiological models of TSEs (see, e.g. Anderson *et al.*, 1996; Stekel *et al.*, 1996) have been based mainly on a phenomenological description of the disease. Laurent's and similar models, because of their simplicity, might be used instead as a building brick in a structured epidemiological model consisting of a collection of different individuals, each being characterized by a set of biochemical and physiological parameters. This would, however, require two crucial steps. First, it would be necessary to go from the local cellular level to the CNS level so as to derive incubation times. This would require the use of spatial models with the problems we described above. Second, a key point in an epidemiological model of this sort would be whether vertical transmission of the disease between a female and its progeny is possible (Butler, 1996). This occurrence of vertical transmission has recently been evidenced by Donnelly *et al.* (1997) and Wilesmith *et al.* (1997), but whether there is a relationship between the mother's and the progeny's prion protein dynamics remains uncertain. Moreover, we do not know whether the transmission could occur as soon as the cells of the brain are in a pathogenic state or only once the neurological dysfunction has appeared. Despite these uncertainties, there is no doubt, in our opinion, that a model coupling the individual with the population level would be a major step towards

testing specific hypotheses on the disease spread and building a bridge between laboratory data and the epidemiological evidence.

The authors are very grateful to Renato Casagrandi, for his assistance in conducting bifurcation analysis, and two referees, whose comments and suggestions were greatly helpful in revising the article. The authors acknowledge the support of Ecole Normale Supérieure, Paris, France.

REFERENCES

- AGUZZI, A. (1996). Between cows and monkeys. *Nature* **381**, 734–735.
- ANDERSON, R. M., DONNELLY, C. A., FERGUSON, N. M., WOOLHOUSE, M. E. J., WATT, C. J., UDY, H. J., MAWHINNEY, S., DUNSTAN, S. P., SOUTHWOOD, T. R. E., WILESMITH, J. W., RYAN, J. B. M., HOINVILLE, L. J., HILLERTON, J. E., AUSTIN, A. R. & WELLS, G. A. H. (1996). Transmission dynamics and epidemiology of BSE in British cattle. *Nature* **382**, 779–788.
- BENDHEIM, P. E., BARRY, R. A., DE ARMOND, S. J., STITES, D. P. & PRUSINER, S. B. (1984). Antibodies to a scrapie prion protein. *Nature* **310**, 418–422.
- BORCHELT, D., SCOTT, R., TARABOULOS, A., STAHL, N. & PRUSINER, S. B. (1990). Scrapie and cellular prion protein differ in their kinetics of synthesis and topology in cultured cells. *J. Cell. Biol.* **110**, 743–752.
- BROWN, D. R., QIN, K., HERMS, J. W., MADLUNG, A., MANSON, J., SROME, R., FRASER, P. E., KRUCK, T., VON BOHLEN, A., SCHULZ-SCHAEFFER, W., GLESE, A., WESTAWAY, D. & KRETZSCHMAR, H. (1997). The cellular prion protein binds copper *in vivo*. *Nature* **390**, 684–687.
- BRUCE, M. E., WILL, R. G., IRONSIDE, J. W., MCCONNELL, I., DRUMMOND, D., SUTTIE, A., MCCARDE, L., CHREE, A., HOPE, J., BIRKETT, C., COUSENS, S., FRASER, H. & BOSTOCK, C. J. (1997). Transmissions to mice indicate that “new variant” CJD is caused by the BSE agent. *Nature* **389**, 498–501.
- BÜELER, H., AGUZZI, A., SAILER, A., GREINER, R. A., AUTENRIED, P., AGUET, M. & WEISSMANN, C. (1993). Mice devoid of PrP are resistant to scrapie. *Cell* **73**, 1339–1347.
- BUTLER, D. (1996). BSE maternal transmission may be released soon. *Nature* **381**, 724.
- CAUGHEY, B. & CHESEBRO, B. (1997). Prion protein and the transmissible spongiform encephalopathies. *Trends Cell Biol.* **7**, 56–62.
- DE ARMOND, S. J., JENDROSKA, K., YANG, S.-L., TARABOULOS, A., HECKER, R., HSIAO, K., STOWRING, L., SCOTT, M. & PRUSINER, S. B. (1992). Scrapie prion protein accumulation correlates with neuropathology and incubation times in hamsters and transgenic mice. In: *Prions Diseases of Humans and Animals* (Prusiner, S. B., Collinge, J., Powell, J. & Anderton, B., eds), pp. 483–496. London: Ellis-Horwood.
- DOLTON, D. C., MCKINLEY, M. P. & PRUSINER, S. B. (1982). Identification of a protein that purifies with the scrapie prion. *Science* **218**, 1309–1312.
- DONNELLY, C. A., FERGUSON, N. M., GHANI, A. C., WILESMITH, J. W. & ANDERSON, R. M. (1997). Analysis of dam-calf pairs of BSE cases: confirmation of maternal risk enhancement. *Proc. Roy. Soc. Lond. B. Biol. Sci.* **264**, 1647–1656.
- EIGEN, M. (1996). Prionics or the kinetic basis of prion diseases. *Biophys. Chem.* **63**, A1–A18.
- GAJDUSEK, D. C. (1977). Unconventional virus and the origin and disappearance of Kuru. *Science* **197**, 943–960.
- GRIFFITH, J. S. (1967). Self-replication and Scrapie. *Nature* **215**, 1043–1044.
- HILL, A. F., DESBRUSLAIS, M., JOINER, S., SIDLE, K. C. L., GOWLAND, I. & COLLINGE, J. (1997). The same prion strain causes VCJD and BSE. *Nature* **389**, 448–450.
- JARRET, J. T. & LANSBURY, P. T. (1993). Seeding “one dimensional crystallization” of amyloid: a pathogenic mechanism in Alzheimer’s disease and scrapie? *Cell* **73**, 1055–1058.
- KACSER, J. & SMALL, J. R. (1996). How many phenotypes can derive from one genotype? *J. theoret. Biol.* **182**, 209–218.
- KHIBNIK, A. I., KUZNETSOV, Yu. A., LEVITIN, V. V. & NIKOLAEV, E. V. (1993). Continuation techniques and interactive software for bifurcation analysis of ODEs and iterated maps. *Physica D* **62**, 360–371.
- KOCISKO, D. A., COME, J. H., PRIOLA, S. A., CHESEBRO, B., RAYMOND, G. J., LANSBURY, P. T. & CAUGHEY, B. (1994). Cell-free formation of protease-resistant prion protein. *Nature* **370**, 471–474.
- KOCISKO, D. A., PRIOLA, S. A., RAYMOND, G. J., CHESEBRO, B., LANSBURY, P. T. & CAUGHEY, B. (1995). Species specificity in the free-cell conversion of prion to protease resistant forms: A model for the scrapie species barrier. *Proc. Nat. Acad. Sci. U.S.A.* **92**, 3923–3927.
- KUZNETSOV, Y. A. (1995). *Elements of Applied Bifurcation Theory*. New York: Springer-Verlag.
- LAURENT, M. (1996a). Les maladies à prion: l’hypothèse de la “protéine seule” et ses conséquences dynamiques. *Médecine/sciences* **12**, 774–785.
- LAURENT, M. (1996b). Prion diseases and the “protein only” hypothesis: a theoretical dynamic study. *Biochem. J.* **318**, 35–39.
- LAURENT, M. (1998). Bistability and the species barrier in prion diseases: stepping across the threshold or not. *Biophys. Chem.* **72**, 211–222.
- LAURENT, M. & JOHANNIN, G. (1997). Molecular clues to pathogenesis in prion diseases. *Histol. Histopathol.* **12**, 583–594.
- MASEL, J., JANSEN, V. A. A. & NOWAK, M. A. (1999). Quantifying the kinetic parameters of prion replication. *Biophys. Chem.* **77**, 139–152.
- MEYER, R. F., MCKINLEY, M. P., BOWMAN, K. A., BRAUNFELD, M. B., BARRY, R. A. & PRUSINER, S. B. (1986). Separation and properties of cellular and scrapie prion proteins. *Proc. Nat. Acad. Sci. U.S.A.* **83**, 2310–2314.
- NOWAK, M. A., KRAKAUER, D. C., KLUG, A. & MAY, R. M. (1998). Prion infection dynamics. *Integrative Biol.* **1**, 3–15.
- OESCH, B., WESTAWAY, D., WÄLCHLI, M., MCKINLEY, M. P., KENT, S. B. H., AEBERSOLD, R., BARRY, R. A., TEMPST, P., TEMPLLOW, D. B., HOOD, C. E., PRUSINER, S. B. & WEISSMANN, C. (1995). A cellular gene encodes scrapie PrP 27-30 protein. *Cell* **40**, 735–746.
- PAYNE, R. J. H. & KRAKAUER, D. C. (1998). The paradoxical dynamics of prion disease latency. *J. theoret. Biol.* **191**, 345–352.
- PRUSINER, S. B. (1982). Novel proteinaceous infectious particles cause scrapie. *Science* **216**, 136–144.
- PRUSINER, S. B. (1991). Molecular biology of prion diseases. *Science* **252**, 1515–1522.

- PRUSINER, S. B., MCKINLEY, M. P., GROTH, D. F., BOWMAN, K. A., MOCK, N. I., COCHRAN, S. P. & MASIAZ, F. R. (1981). Scrapie agent contains a hydrophobic protein. *Proc. Nat. Acad. Sci. U.S.A.* **78**, 6675–6679.
- PRUSINER, S. B., SCOTT, M., FOSTER, D., PAN, K. M., GROTH, D., MIRANDA, C., TORCHIA, M., YANG, S. L., SERBAN, D., CARLSON, G. A., HOPPE, P. C., WESTAWAY, D. & DE ARMOND, S. J. (1990). Transgenic studies implicate interactions between homologous PrP isoforms in scrapie prion replication. *Cell* **63**, 673–686.
- STEKEL, D. J., NOWAK, M. A. & SOUTHWOOD, T. R. E. (1996). Prediction of future BSE spread. *Nature* **381**, 119.
- WEISSMANN, C. (1994). Molecular biology of prion diseases. *Trends Cell. Biol.* **4**, 10–14.
- WEISSMANN, C. (1995). Yielding under the strain. *Nature* **375**, 628–629.
- WILESMITH, J. W., WELLS, G. A., RYAN, J. B., GAVIER-WIDEN, D. & SIMMONS, M. M. (1997). A cohort study to examine maternally associated risk factors for bovine spongiform encephalopathy. *Vet. Rec.* **141**, 239–243.
- WILLE, H., ZHANG, G., BALDWIN, M. A., COHEN, F. E. & PRUSINER, S. B. (1996). Separation of scrapie prion infectivity from amyloid polymers. *J. Mol. Biol.* **259**, 608–621.